D4.5 Material specific dose-response functions and validation required in the CH vulnerability assessment

Deliverable number	**D4.4**
Deliverable title	Material specific dose-response functions and validation required in the CH vulnerability assessment
Nature1	**R**
Dissemination Level [2]	**PU**
Author (email) Institution	**Chiara Coletti (chiara.coletti@unipd.it)** **Luigi Germinario (luigi.germinario@unipd.it)** **Claudio Mazzoli (claudio.mazzoli@unipd.it)** **UNIPD**
Editor (email) Institution	**Claudio Mazzoli (claudio.mazzoli@unipd.it)** **UNIPD**
Leading partner	**UNIPD**
Participating partners	
Official submission date:	**31/08/2021**
Actual submission date:	**07/09/2021**

[1] **R**=Document, report; **DEM**=Demonstrator, pilot, prototype; **DEC**=website, patent fillings, videos, etc.; **OTHER**=other

[2] **PU**=Public, **CO**=Confidential, only for members of the consortium (including the Commission Services), **CI**=Classified, as referred to in Commission Decision 2001/844/EC

Modifications Index	
27/08/2021	0.1 First draft by the Author
31/08/2021	0.2 Final version edited by the WP leader

This work is a part of the HYPERION project. HYPERION has received funding from the European Union's Horizon 2020 research and innovation programme under grant agreement no 821054.

ACRONYMS AND ABBREVIATIONS

CH	Cultural Heritage
DRF	Dose-response function
OM	Optical Microscopy
XRPD	X-ray Powder Diffraction
MIP	Mercury Intrusion Porosimetry
CM	Confocal Microscopy

Table of Contents

Executive Summary

Although several studies have been carried out about the complexity of the physical, chemical, mineralogical, petrographic and biological aspects of the deterioration of stone materials, at present there is no definitive achievement on the understanding and quantification of climate change effects on stone surface recession.
HYPERION results are filling this gap, by improving our knowledge on measurable parameters influencing deterioration rate, especially those related to the environment (e.g., temperature, relative humidity, precipitation amount, pollutant agents, etc.). Inadequacy of existent dose-response deterioration equations strongly limit the applicability to real specific situations. Therefore, a deeper knowledge of surface recession related to the petrographic features of stones is fundamental to define new reliable dose-response functions. Laboratory tests, in controlled conditions and reproducing different environmental conditions (in particular, using different rainwater compositions, which strongly affect the damage of carbonate rocks), allow quantifying the surface recession rate phenomena and the prediction of future scenarios. The optimisation of dose-response functions can actually be a significant tool for mitigating climate change effects on cultural heritage. In order to reach this goal, this Deliverable (D4.5) aims to measure the recession rate of eleven carbonate rocks widely used in the cultural heritage of Italy. This increases the number of stone types adopted in the HYPERION project, in order to cover the largest range of types of limestones (e.g. different in grain size, composition, porosity) and to obtain the largest case study to be applied in different contexts. These stones were subjected to accelerated ageing tests in an environmental test chamber for simulating the wetting effect of rainwater, using two different water compositions corresponding to two different rainwaters (with pH≈6 and pH≈7). Bulk stone recession is evaluated considering sample weight loss as a function of the number of wetting cycles. Moreover, direct measurements of recession are performed by Confocal Microscopy (CM), which allowed 3D reconstruction of the stone surface and evaluation of differential recession as a function of calcite grain size.

1. Introduction

Water is a first-order cause of stone damage because it can interact in different ways with the stone material causing different patterns of stone decay.

The potential threat of acid rain on cultural heritage assets, especially those made of carbonate rocks, is widely studied in the literature and it is a major concern in conservation science. However, we are far from a satisfactory understanding of the interaction among the different parameters controlling stone recession, therefore our ability in predicting trends of future decay is still too weak to be reliably used by stakeholders and decision makers. This is the main focus of this Deliverable (D4.5).

In order to achieve these objectives, we increased our stones dataset, considering and refining data from a larger set of stones from a previous work (Salvini, 2017, PhD Thesis).

1.1 Background

In the last 40 years various researchers tried to assess and quantity the degradation phenomena of stone materials by considering changes in their surface topography (recession) and/or loss of material (e.g., disintegration, detachments).

Large part of these contributions had the aim of testing the decay of carbonate rocks under specific environmental conditions reproducing as closely as possible the chemical characteristics of natural rainfall, often using environmental test chambers in order to simulate natural conditions.

The main environmental parameters considered in dose-response functions (DRF) are i) the concentration of specific pollutants in the atmosphere, ii) the [H+] concentration in rainwater, iii) the rainfall, and iv) the temperature.

Lipfert (1989) identified in dissolution, air pollution, and acid rains the three main factors of damage for limestones. He set the Lv (Lipfert value) at 18.8 µm m^{-1} (microns of recessed surface per meter of precipitation), based on the solubility of calcite in equilibrium with 330 ppm of CO_2 and quantified the loss of material as annual surface recession per meter of precipitation. Reddy et al. (1986) normalized the annual surface recession as annual rainfall, while Baedecker and Reddy (1993) designed another equation to define the material loss based on the combined effect of temperature and concentration of hydrogen ions.

Webb et al. (1992) estimated the weight loss of material per unit surface considering the influence of various pollutant agents, the rainfall, and the acid ionic concentration. Other authors considered the time of wetting (TOW), the period of time when the relative humidity is higher than 80% and the temperature is above 0 °C, as important parameter to study the degradation effect due to the presence of water. Kucera and Fitz (1995) derived a new equation of the total loss (expressed in g/m^2) based on run-off tests (which lasted 4 years), while the surface recession of marble (per meter of rainfall) has been modeled with field measurements by Yerrapragada et al. (1996), and it was found that the loss of surface due to the impact of rain droplets was seven times greater than that caused by the black crust formation.

Recently, Delalieux et al. (2002) modified previous equations in order to express the material loss as a linear recession measured in microns, and defined a new equation considering five different locations, collecting more than 30 thousand data over three years of measurements, interpreting them using regression mathematical models in order to identity the significant variables to implement in the functions. Lan et al. (2005) studied the effect of stone exposition to sheltered and unsheltered environments after on-site experiments.
Kucera and his research group (Kucera et al. 2007) investigated the effect of different pollutants on materials, including carbonate rocks, in the frame of international exposure programs (MULTI-ASSESS Project 2007). They proposed a damage function for carbonate rocks, considering the increasing values of SO_2 and the increasing values of nitrates, HNO_3 and particulate matter, due to the increase of vehicular traffic in the last decades in Europe. Results indicated that SO_2 is the predominant factor of decay in multi-pollutant areas.
Livingston (2016) calculated the acid neutralization path in the pH range 3.5-6 and the effect of dry deposition, describing material loss in terms of amount of Ca^{2+} ion released by the material applying the electroneutrality condition between the solution chemistry of rainfall and runoff. Martinez-Martinez et al. (2017) analyzed stones in aggressive environment counting the number of years of natural aging required to achieve the same state of erosion in the stone after artificial tests.
Despite the rich literature, at present there is no definitive achievement on the understanding and quantification of climate change effects on the surface recession.

1.2 Purpose and scope

In the last years, Salvini (2017) studied selected Italian carbonate stones simulating the wetting effect of rainwater in environmental chambers and demonstrated that a careful evaluation of petrographic features, such as grain size, porosity, pore-size distribution, mineralogy (e.g., content in clay minerals, sulfurs, etc.) also have an important role in surface recession rate. We updated results from this work in order to better refine the dose-response functions in order to reproduce the largest possibility of limestone used in CH in relation to different rain water compositions.

The selected stones were subjected to accelerated ageing tests in an environmental test chamber for simulating the rainwater effect.

Recession was evaluated in two different ways:

1. Bulk stone recession is evaluated considering sample weight loss as a function of the number of wetting cycles.
2. Direct measurements are performed by Confocal Microscopy (CM), which allow 3D reconstruction of the stone surface and evaluation of differential recession as a function of calcite grain size.

Regarding the selection of materials to be subjected to accelerated aging tests, eleven carbonate rock types (see Table 1 and Fig. 1) characterized by a large range of

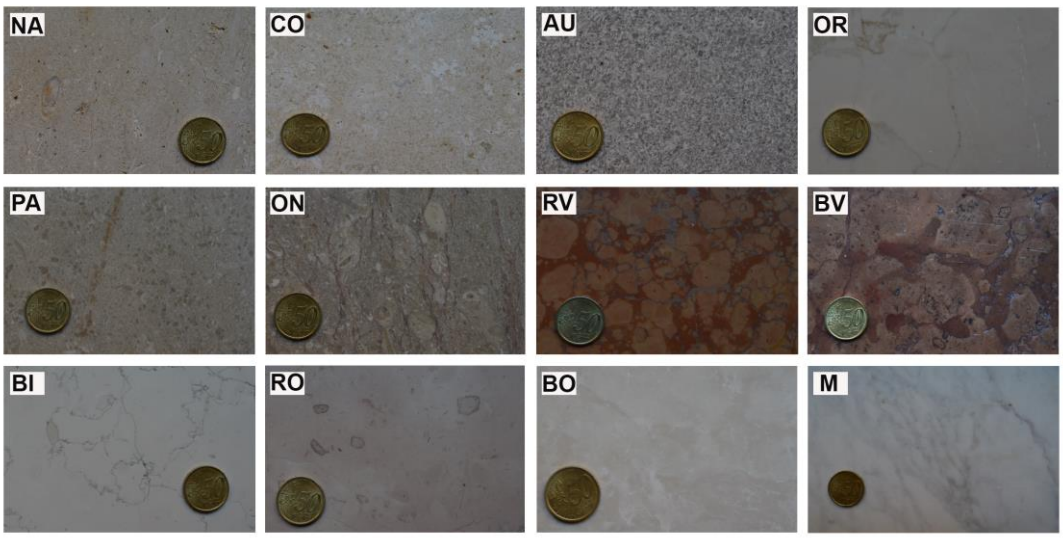

Figure 1: Macroscopic images of the selected limestones and the Carrara marble (M) as reference.

Table 1. Summary of the principal lithological classifications, geological formations, and ages of the carbonate rocks considered in this research.

Sample	Abbr.	Folk Class. [93]	Dunham Class. [94]	Geological Formation	Geological Age
Carrara Marble *	M	---	Crystalline carbonate	Tuscan Nappe	Cretaceous
Botticino Stone *	BO	Dolomitic Micrite	Crystalline carbonate	Corna Formation	Upper – Lower Jurassic
Brown Verona Stone	BV	Biomicrite	Wackestone	Rosso Ammonitico Veronese	Middle – Late Jurassic
Red Verona Stone *	RV	Biomicrite	Wackestone	Rosso Ammonitico Veronese	Middle – Late Jurassic
Chiampo Paglierino Stone	PA	Biomicrite	Packstone/Grainstone	Nummulitic Limestone	Middle Eocene
Chiampo Ondagata Stone	CO	Biomicrite	Packstone/Grainstone	Nummulitic Limestone	Middle Eocene
Pink Asiago Stone	RO	Biomicrite	Wackestone	Majolica Veneta	Lower Cretaceous
Nanto Stone	NA	Biomicrite	Packstone	Nummulitic Limestone	Lower Eocene
Costozza Stone *	CO	Biomicrite	Packstone	Calcareniti di Castelgomberto	Oligocene
Aurisina Stone	AU	Biomicrite	Packstone	Trieste Karst Limestone	Cretaceous
Orsera (Istria) Stone *	OR	Micrite	Mudstone	Unity of External Dinarides	Jurassic

**** = lithologies of Hyperion dataset***

petrographic and textural features have been considered among those most frequently used in the built environment in Italy.
In addition, Carrara marble has also been selected because most of the previous studies on the recession rate of carbonate rocks are mainly based on measurements performed on marbles, and often on Carrara marble.

1.3 Analytical methodology

Optical microscopy (OM)

Thin sections were observed using a Zeiss® Axio Scope.A1 optical microscope (OM) coupled with an Axio CamMRC5 (Department of Geosciences, Padova) to determine their petrographic and textural features.

X-ray Powder Diffraction (XRPD)

The mineralogical composition of the studied samples was identified using a PANalytical θ-θ diffractometer equipped with a Cu X-ray tube operating at 40 kV and 40 mA, a sample spinner, a Ni filter and a solid-state detector (X'Celerator).

Mecrury Intrusion Porosimetry (MIP)

MIP was performed using a PoreMaster 33 system (Quantachrome Instruments ®) with the following parameters: the sample cell is 1.0 × 3.0 cm in size and 2 cm3 in volume, pressure range is 0.5–33.000 psi, the contact angle (θ) of mercury is 140°, and surface tension (σ) of mercury is 0.48 N/m (480 dyn/cm), pore size range is from 0.0064 to 950 µm. Dry density of the materials was measured through picnometer Ultrapic 1200. The considered value of density was the mean of 10 measures.

Accelerated aging tests

Preparation of samples for the accelerated ageing tests

One sample from the selected eleven rock types (dimension ≈ 2 x 2 x 1 cm) has been prepared to be subjected to accelerated aging tests in an environmental test chamber. Stainless steel washers were cut in two halves, attached to the opposite sides of each specimen with Araldite 2020. These metal parts are resistant to decay, and therefore they may be used as reference quotes in the evaluation of stone recession. The surface of the samples was lapped using sandpaper with a grit of 1200.

Artificial rainwater used for the aging tests

Accelerating aging tests consisted in a sequence of immersion and emersion cycles within two different solutions artificially prepared to be as similar as possible to the rainwater wetting city of Bologna (Panettiere et al. 2000), with pH≈7, and Stresa (Rogora et al. 2004), with pH≈ 6. The ionic concentrations of these two types of water are reported in Table 2. The necessary ions were introduced in the form of compounds: $CaCO_3$, $CaCl_2$, KCO_3, Na_2SO_4, $Mg(OH)_2$, H_2SO_4(96%), NaCl, Ca_5O_4, $MgSO_4 \cdot 7H_2O$, $[NH_4]2SO_4$, $[NH_4]NO_3$, KNO_3, NH_3(21%), HNO_3(98%).

Table 2. Composition of the two types of water used for the accelerated aging test. Concentration values exposed here are in mmol/45 l, which is the total volume of water prepared to be located within the environmental test chamber.

	Na^+	K^+	Mg^{2+}	Ca^{2+}	Cl^-	SO_4^{2-}	HCO_3^-	NH_4^+	NO_3^-	H^+
Bologna	1.575	0.495	0.540	3.465	1.755	1.575	4.23	--	--	--
Stresa	0.810	0.135	0.360	2.88	0.405	3.69	1.89	2.34	1.80	0.675

The environmental test chamber setting

Aging tests have been performed using a benchtop Suntest CPS+ Xenon exposure system (Department of Chemical Sciences, University of Padova) equipped with a Xenon Arc Lamp and an immersion system to completely cover the specimens with water. This equipment can contain 45 liters of water. It is also equipped with a parabolic reflector, a photodiode, and a ventilation system.

The samples were subjected to 240 cycles under dry (emersion phase) or wet (immersion phase) conditions table 3.

Table 3. Environmental test chamber parameters for the accelerated aging cycles performed.

Phase	$T_{(water)}$	$T_{(ref\ surf)}$	Irradiation	Time
Immersion	25°C	40°C	300 W/m^2	60 min.
Emersion	No water	70°C	500 W/m^2	180 min.

Recession measurements

1) Bulk stone recession

Material loss of the different specimens has been evaluated after 54, 140, and 240 cycles with respect to the original stone surface. Stone surface recession has been evaluated in different ways. The first one consisted in the measurement of the weight loss of the sample using an analytical scale (accuracy 0.0001 g). The weight loss was then converted to volume loss dividing by the stone density and then to linear recession dividing the volume loss by the external surface measured using a caliper (accuracy 0.01 mm).

2) Direct measurements

Topographic surface of a specific area on each sample was measured after 54, 140 and 240 cycles, and compared to the portion of the same surface acquired before the aging tests. The method consisted in the three-dimensional surface description using an Olympus Lext OLS4000 confocal laser microscope (Department of Geosciences, University of Padova). For each sample, a matrix of 6x6 scans was acquired at a magnification of 200x. Each scan consisted of a number of acquisition layers merged by the LEXT acquisition software, the number of which strongly depends on the surficial roughness of the samples and affects the total acquisition time. Each acquisition resulted in a surface topographic map of about 3x3 mm, with a lateral resolution of 1 micron, and a vertical submicrometric resolution. For each sample, four different topographic maps were produced on the same area, one before the attack and one after each set of aging cycles (i.e., after 54, 140, and 240 cycles). These data were then exported as *.csv files and processed by the Matlab® software package to

generate point clouds to be successively imported in ArcMap® computer program. For computational reasons, the point clouds were subsamples, reducing lateral resolution to 5 microns. This software allowed building a reference surface for each of the topographic maps taking the metal altitude as a reference. Recession in each specific point or area of interest was then obtained by difference from the reference surfaces.

2. Results and discussion

2.1 Petrographic characterization

The results of the petrographic characterization, including information on the mineralogical composition, porosimetric properties, and density, are summarized in Table 4. Further information on the texture are in Table 5, presenting the grain size measurements performed on thin section under the optical microscope.

Table 4: Results of the XRPD, MIP, and densitometry. Mineral abbreviations: Cal = calcite; Qtz = quartz; Dol = dolomite, Mg-Cal=Mg-Calcite, Ms = muscovite; Ill = Illite; Plg M = palygorskyte M. Percentages obtained with RIR method.

Sample ID	XRPD composition	MIP Porosity > 0.006 µm (%)	MIP Ø max (µm)	Density (g/cm^3)
RO	98% Cal, 2% Qtz	3.53	216.47	2.688±0.008
AU	100% Cal	4.61	272.89	2.705±0.007
BV	94% Cal, 4% Ill, 2% Qtz	0.10	4.04	2.720±0.005
BO	57% Cal, 43% Dol	1.73	235.34	2.766±0.004
ON	66% Cal, 34% Mg-Cal, traces Plg M	1.04	216.47	2.707±0.007
M	100% Cal, traces Ms	1.00	215.56	2.741±0.002
NA	95% Cal, 5% Ill	27.18	371.77	2.789±0.008
OR	100% Cal	0.40	211.13	2.711±0.007
PA	61% Cal, 38% Mg-Cal, 1% Plg M	0.34	221.52	2.708±0.004
RV	100% Cal	0.25	379.47	2.729±0.005
CO	100% Cal	28.52	221.52	2.737±0.004

Table 5: Grain size of different textural elements measured on thin section under the optical microscope. The values marked with * were calculated averaging at least 100 measures, or 1000 for marble.

Sample ID	Textural element	Grain size (µm)
RO	Micrite	<0.1–0.3
	Coarse-grained micrite	1–2, or 3–5 (inside bioclasts)
	Bioclasts	44*
AU	Fine micrite	<1
	Coarse-grained micrite	5–10
	Sparry calcite	20
	Bioclasts	Up to 1000-2000
BV	Micrite	1
	Coarse-grained micrite	5–10
	Sparry calcite	20
	Bioclasts	Ostracods: 30* (thickness); Ooids: 85*
BO	Micrite	2
	Coarse-grained micrite	5-10
	Bioclasts	30
	Dolomite	127*
ON	Micrite	<1
	Coarse-grained micrite	5
	Sparry calcite	25* (bulk rock)–40* (inside bioclasts)
	Bioclasts	Up to cm size
M	Coarse calcite	155*
NA	Micrite (Bioclasts)	1–4
	Micrite	10
	Sparry calcite	35
	Bioclasts (Echinoderms)	300-500
OR	Micrite	3–5
	Sparry calcite	40*
PA	Micrite	<1
	Coarse-grained micrite	5
	Sparry calcite	45* (inside bioclasts)
	Bioclasts	Up to 2000
RV	Micrite	1
	Coarse-grained micrite	5–10
	Bioclasts	Ostracods: 30* (thickness); Ooids: 107*
CO	Sparry calcite	5–10
	Bioclasts	500 or more
	Micrite	<1

2.2 Surface recession

2.2.1 Experimental findings

The recession values determined with different techniques are reported in Table 6.

Firstly, the recession is always dependent on the water composition used during the ageing cycles, in particular on the pH, which is about 6 for Stresa and 7 for Bologna. Consequently, the samples immerged in the Stresa water with lower pH always show higher values of total recession.

Secondly, the recession changes based on the stone and its textural characteristics, in particular grain size. For example, comparing two materials with similar (low) porosity, Carrara marble is characterized by a quite homogeneous coarse grain size, whereas Orsera is a micritic limestone. Recession is clearly higher in Orsera, i.e., about 20-50% more than the recession measured on Carrara Marble. Aurisina shows intermediate recession values instead: although its grain size is relatively coarse, is still significantly finer than in Carrara marble. Another illustrative case is represented by the recession of Botticino, which has a dolomite content of 46%: the linear surface recession of the calcitic portion is significantly higher than what measured in the dolomitic portion, since calcite is much more soluble than dolomite.

A third systematic correlation is found between recession rate and presence of expansive clay minerals. Nanto, Red Verona, and Brown Verona all have a noticeable content of clay minerals, and are all characterized by the highest recession rates.

No evident correlation was found with porosity instead.

Table 6: Recession values (µm) obtained from weight loss measurements and by confocal microscopy.

Sample ID	Bologna						Stresa					
	Weight loss			Confocal microsc.			Weight loss			Confocal microsc.		
	Cycles			Cycles			Cycles			Cycles		
	54	141	240	54	141	240	54	141	240	54	141	240
RO	-4.81	-9.72	-12.5	--	--	16.90	-10.28	-18.31	-24.6	10.14	20.92	31.38
AU	-3.35	-8.72	-11.3	6.42	14.12	17.03	-8.73	-15.91	-21.7	8.49	18.87	33.00
BV	-2.25	-8.17	-10.7	5.66	10.70	14.34	-5.13	-10.32	-18.9	5.53	--	31.61
BO	-4.37	-9.68	-12.1					-11.33	-16.1	8.74		33.94
ON	-5.26	-11.18	-13.8	6.10	14.61	24.42	-7.10	-13.80	-20.6	7.28	24.43	32.98
M	-3.29	-8.37	-11.1	5.52	10.42	13.03	-6.38	-12.44	-17.4	10.93	18.89	24.42
NA	-3.50	-10.19	-14.3	--	8.20	14.29	-6.40	-13.46	-20.4	9.72	--	22.89
OR	-8.05	-16.96	-20.2	7.87	14.80	22.07	-6.06	-17.55	-26.3	14.70	28.40	34.55
PA	-4.80	-11.31	-13.9	6.19	--	15.69	-6.05	-14.09	-20.6	7.44	21.91	31.78
RV	-6.03	-12.83	-15.7	5.29	14.81	12.09	-4.84	-11.58	-21.3	9.48	23.46	28.47
CO	-4.79	-12.22	-16.2	3.06	9.77	18.05	-5.68	-14.21	-21.9	6.21	18.80	28.93

Image analysis of the stone surface supported by confocal microscopy allowed quantifying the different recession rates for different textural elements. Fig. 2 and 3 show two representative 3D surface models obtained by confocal microscopy samples of Chiampo Paglierino (CP) and Botticino (BO). In the case of Chiampo Paglierino, evolution of the stone surface during the ageing shows a clear differential recession of the bioclasts, which remain in relief in respect to the surrounding fine-grained micrite and the sparry calcite observed in veins or along bioclast rims. In the case of Botticino, the dolomite crystals "rise" from the receding surrounding micrite; after 240 ageing cycles with Stresa water, the former show an average recession lower than 3 µm, while the latter reaches values of about 33 µm (fine-grained micrite) and 29 µm (coarse-grained micrite). These values are in agreement with the linear recession estimated from weight loss measurements (Table 6), except for Orsera (for which the average recession calculated by confocal microscopy is 29.12 µm, whereas the weight loss measurements give a value of 14.3 µm).

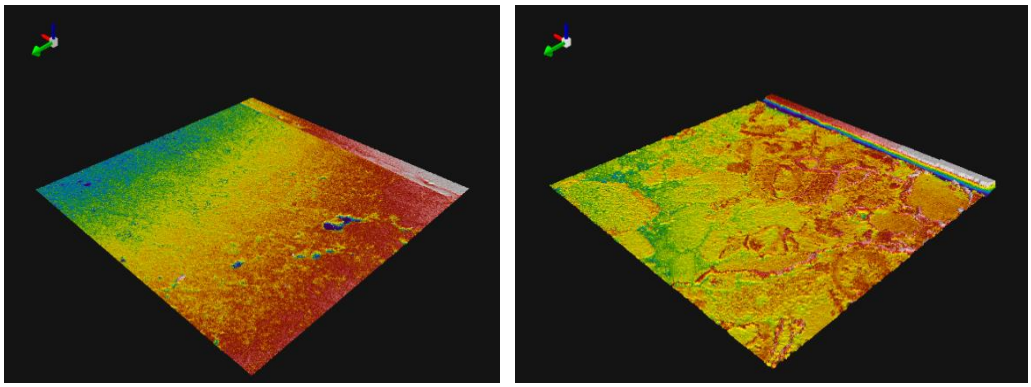

Figure 2: 3D surface model for a sample of Chiampo Paglierino Stone (P02) before aging (left) and after 240 aging cycles in Stresa water (bright).

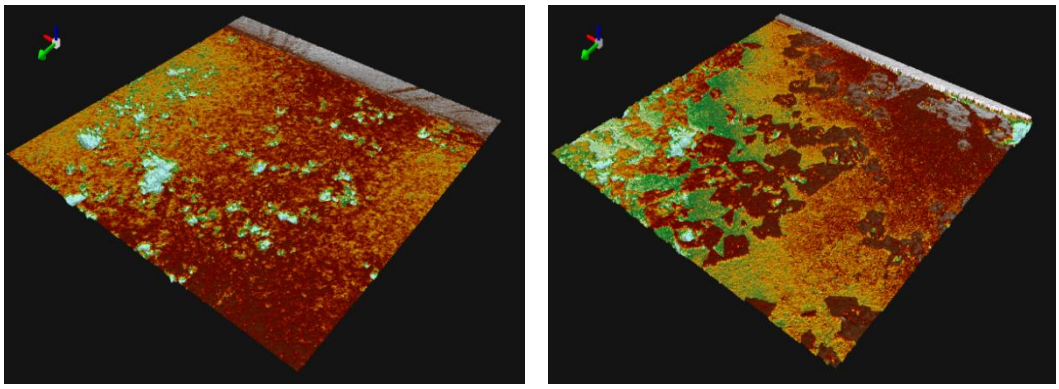

Figure 3: 3D surface model for a sample of Botticino Stone (BO02) before aging (left) and after 240 aging cycles in Stresa water (right).

From a general point of view, the image analysis suggests that coarse-grained sparry calcite shows a recession being half on average of the recession of fine-grained micrite. Slightly lower recession values were obtained for coarse-grained micrite. Finally, bioclast recession covers a broad spectrum of values, which are intermediate

between those of sparry calcite and coarse-grained micrite (Table 8). This further supports the observed direct control of grain size on the recession rate. The relevant aggregated data are displayed in Fig. 4, showing clear trends of positive correlation between recession and grain size.

Table 8: Summary of the recession values (in µm) measured after the processing of the 3D models.

Sample ID	Micrite		Coarse-grained micrite		Sparry calcite		Bioclasts		Dolomite	
	Bologna	Stresa	Bologna	Stresa	Bologna	Stresa	Bologna	Stresa	Bologna	Stresa
BO	-17.23	-33.00	-14.33	-29.01	--	--	-17.22	--	-2.33	-0.50
ON	-21.24	-39.78	-18.21	-37.32	-8.82	-24.53	-18.09	-30.20	--	--
M	--	--	--	--	-13.03	-26.12	--	--	--	--
NA	-20.36	-29.70	-10.67	--	-5.73	-13.17	-13.06	-20.37	--	--
OR	-33.61	-35.51	--	--	-7.02	-19.16	--	--	--	--
PA	-21.54	-36.57	-17.42	--	-10.51	-17.55	-13.64	-26.33	--	--
RO	19.15	-34.10	-16.54	--	--	--	-11.31	-20.61	--	--
AU	-21.81	--	-18.13	-40.77	-11.36	-20.23	-13.64	-26.94	--	--
BV	-17.28	-35.75		-33.46	-7.38	-23.09	-8.83	-26.80	--	--
RV	-21.36	-29.98	--	--	--	--	-10.98	-21.28	--	--
CO	-21.88	-30.82	--	--		-16.65	-13.07	-18.85	--	--
Mean	**-22.80**	**-36.18**	**-15.16**	**-29.01**	**-8.02**	**-16.12**	**-14.98**	**-30.23**	**-2.33**	**-0.50**

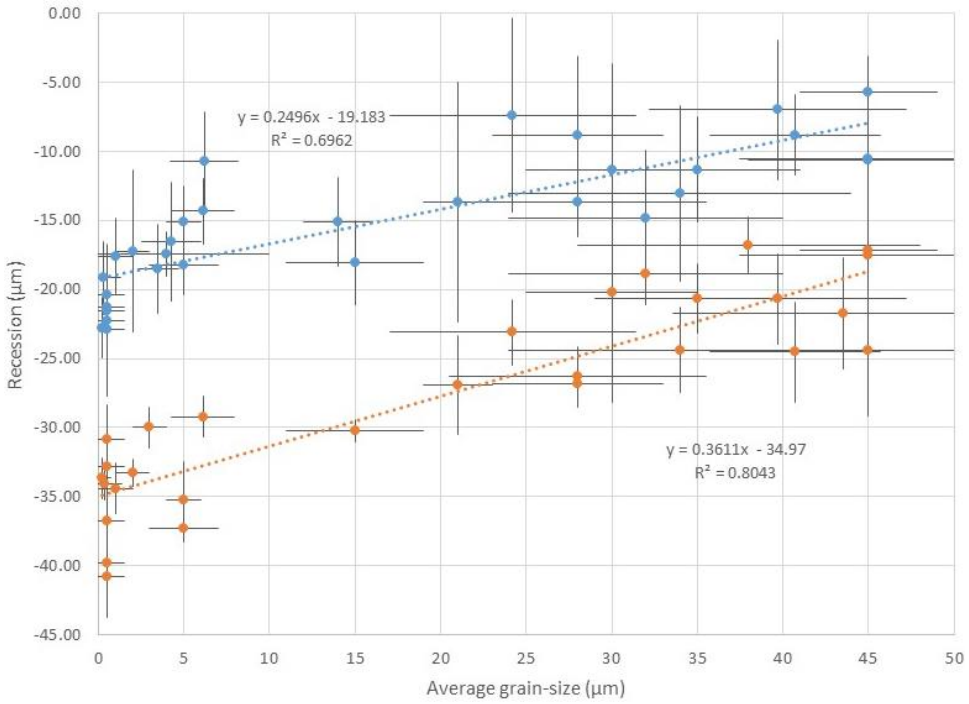

Figure 4: Correlation between average grain size (accounting for the different textural elements) and average recession measured on all the samples after 240 aging cycles with the water from Bologna (blue trend) and Stresa (orange trend).

The last step of data processing was to use existent equations for predicting surface recession of stone (modelled considering marble weathering) (Reddy et al. 1985, Lipfert 1989, Baedecker 1990, Webb et al. 1992, Kucera & Fitz 1995, Delalieux et al. 2002), use them with specific environmental variables, and eventually compare the values obtained. The material considered was Carrara marble. As for the environmental variables, the following assumptions were made, also taking into account the experimental conditions applied during the ageing tests:

- the precipitation amount is equal to 1 m, representing approximately the annual rainfall in numerous cities of northern Italy;
- the concentrations of air pollutants (SO_2, NO_2, O_3) are those actually detected in Padova (source: ARPAV – Regional Agency for the Environmental Prevention and Protection of Veneto)
- the deposition velocity of SO_2 and NO_2 is 0.3 cm/s and 0.1 cm/s, respectively (Lipfert 1989);
- time of wetness is 0.6;
- temperature is 25 °C;
- pH is 6 or 7, depending if the water from Stresa or Bologna is considered;
- SO_4^{2-} concentration is 0.082 mmol/L or 0.035 mmol/L, depending if the water from Stresa or Bologna is considered.

The recession of Carrara marble after 240 ageing cycles experimentally measured by its weight loss was 17.4 µm in the Stresa water and 11.1 µm in the Bologna water (Table 6). These values turn out to be very similar to those calculated applied the Delalieux's equation, i.e., 15.32 µm and 11.57 µm, respectively. This suggests that the 240 cycles in the experimental conditions previously described correspond to a rainfall of about 1 m in natural conditions and exposure.

The other equations gave less concordant results. Lipfert's equation provided the highest recession values (19.76 µm for both the waters), while Reddy's, Baedecker's, Webb's, and Kucera's functions all gave similar values, between 4.9 µm and 6.4 µm.

2.2.2 Correlation coefficient

The dataset obtained during this study is useful for providing a broad perspective on stone recession considering together a number of parameters, that is, grain size, heterogeneity of grain-size distribution, and content in clay minerals. The global effects of these properties (and, possibly, also of porosity) are considered calculating a phenomenological coefficient Φ, which is proposed for obtaining more reliable projections of stone deterioration for different types of carbonate rocks. The coefficient Φ is the ratio between the recession of a given stone material and the recession of Carrara marble in the same ageing conditions (Table 9). Table 10 suggests other similar stone materials for which the coefficient might be used.

In this regard, the applicability of the coefficient Φ was tested considering the equation by Reddy et al. (1985) for estimating the theoretical recession of stone. That equation was applied to a number of different materials for which direct recession

measures are available in the literature. Finally, the theoretical recession was corrected with the coefficient Φ to check if the result would be consistent with the direct measures. Table 11 summarizes the relevant findings.

The coefficient Φ calculated for Nanto stone (1.5) was used for the comparison with the recession data of Portland limestone in highly polluted areas and in the countryside in the UK (Honeyborne & Price 1977), and of a porous limestone in urban environment in Austria (Weber 1985); these materials being characterized by similar textural features if compared to Nanto, in terms of calcite grain size, presence of bioclasts, porosity, and content in clay minerals.

The coefficient Φ calculated for Botticino (0.95), instead, was used for the comparison with the Indiana limestone, which likewise has a noticeable dolomite content (Reddy et al. 1985).

Chiampo stone is similar to a compact limestone studied by Weber (1985), in terms of texture and low porosity. For that, the Chiampo's coefficient Φ (1.15) can be applied.

The comparison between the measured recession rates for all these carbonate rocks and the theoretical recession rate corrected with the coefficient Φ, is satisfactory. Therefore, the proposed coefficient seems to well account for the different petrographic features influencing stone recession rate in the same environmental conditions.

Table 9: Coefficient Φ calculated from the recession values estimated after 240 ageing cycles by weight-loss measurements (WL) and confocal microscope (CM).

Sample ID	Bologna - WL		Bologna - CM		Stresa - WL		Stresa - CM		Mean
	Recession	Φ	Recession	Φ	Recession	Φ	Recession	Φ	Φ
RO	-12.5	1.13	-16.90	1.30	-24.6	1.41	30.85	1.09	**1.23**
AU	-11.3	1.02	-17.46	1.34	-21.7	1.25	27.66	0.98	**1.15**
BV	-10.7	0.96	-14.84	1.14	-18.9	1.09	30.16	1.07	**1.06**
BO	-12.1	1.09		0.00	-16.1	0.93		0.00	**0.50**
CO	-13.8	1.24	-14.42	1.11	-20.6	1.18	30.24	1.07	**1.15**
M	-11.1	1.00	-13.03	1.00	-17.4	1.00	28.21	1.00	**1.00**
NA	-14.3	1.29	-21.94	1.68	-20.4	1.17	23.54	0.83	**1.25**
OR	-20.2	1.82	-21.94	1.68	-26.3	1.51	34.90	1.24	**1.56**
PA	-13.9	1.25	-18.29	1.40	-20.6	1.18	31.98	1.13	**1.24**
RV	-15.7	1.41	-17.20	1.32	-21.3	1.22	28.78	1.02	**1.24**
CO	-16.2	1.46	-18.05	1.39	-21.9	1.26	27.83	0.99	**1.27**

Table 10. Suggested coefficients Φ for various carbonate rocks based on the results presented in this study. These values are also applicable to other stones characterized by similar mineralogical composition, texture, and grain size.

Stone name	Geological classification	Φ	Porosity	Notes	Also suggested for
Carrara	Crystalline carbonate	1.00	Low	Grain size ≈ 100 µm	Naxos, Paros, Aghia Marina, Pentelico
Botticino	Dolomitic Micrite/ Cryst. carbonate	0.95	Low	Calcite 57%, Dolomite 43%	Indiana limestone
Verona	Biomicrite Wackestone	1.25-1.80	Very Low	High heterogeneity, nodular limestone	Rouge du Roi, Tardos (Hungary), Adneter (Austria), Moneasa (Romania), Rouge Languedoc?
Pink Asiago	Oomicrite/ Wackestone	1.30	Very Low		
Chiampo	Biomicrite/ Grainstone	1.15	Low		Beige of Missolonghi
Vicenza	Biomicrite/ Packstone	1.50	High	Micritized fossils, clay minerals, heterogeneity	Portland, Lecce?, Noto?
Aurisina	Biomicrite/ Packstone	1.10-1.20	Medium	Micritized fossils	
Orsera	Micrite/ Mudstone	1.30	Low	Fine grain size (3 µm)	

Table 11: Application of coefficient Φ to the recession estimates obtained using the equation of Reddy et al. (1985), and comparison with actually measured recession rates (in µm). HP77: Honeyborne & Price (1977); R85: Reddy et al. (1985); W85: Weber (1985).

Ref.	Location	Material	Measured recession	SO_2 (µg/m^3)	Rainfall (m/yr)	[H^+] (mmol/L)	Recession (R85)	Corrected rec. value	Φ
HP77	London	Portland	50.0	140	1	0.15	37.06	55.59	1.5
HP77	Rural, U.K.	Portland	17.0	30	1	0.015	9.22	13.83	1.5
R85	East U.S.	Indiana limestone	7.0	20	1	0.015	8.53	8.10	0.95
W85	Vienna	Porous limestone	26.5	70	1	0.055	17.98	26.97	1.5
W85	Vienna	Compact limestone	20.1	70	1	0.055	17.98	20.68	1.15
W85	Vienna	Marble	18.0	70	1	0.055	17.98	17.98	1.0

3. Conclusions

The previous research on stone weathering has proposed a number of mathematical relations for predicting or indirectly evaluating stone recession rate based on a set of environmental parameters, generally applied to marbles. However, those equations turn out to be less reliable when applied to limestones.

For further exploring this topic, an experimental investigation was conducted to determine the possible correlation between recession of different carbonate rock types and their petrographic features. To that purpose, a series of ageing tests were done in an environmental test chamber simulating the effects of rain, with the same composition of rainwater in the two Italian cities of Bologna (water pH ≈ 7) and Stresa (pH ≈ 6).

Stone recession was calculated on the basis of material weight loss and measured by confocal microscopy, and positively correlated to the grain size of calcite and content of clay minerals. The effect of porosity seemed to be less significant. Based on the relevant datasets, a phenomenological coefficient was calculated, to be applied for estimating the recession of other carbonate rocks with similar textural and mineralogical features.

This Deliverable (D4.5) allows to better define dose-response function and is in support to on-site results in environmental microclimate conditions (D4.3) and for improving HT simulations and SG models in order to predict future risk scenarios.

4. REFERENCES

1. Baedecker P. A. (1990). Effects of acidic deposition on materials. Washington, USA: National Acid Preparation Assessment Program.
2. Baedecker P.A., Reddy M.M., The Erosion of Carbonate Stone by Acid Rain, Journal of Chemical Education 70, 2 (1993) 104-108.
3. Delalieux F., Cardell-Fernandez C., Torfs K., Vleugels G., Van Grieken R., Damage functions and mechanism equations derived from limestone weathering in field exposure. Water, Air, & Soil Pollution, 139(1):75-94 (2002) 75-94. https://doi.org/10.1023/A:1015827031669.
4. Honeyborne D. B., Price C. A. (1977). Air pollution and the decay of limestone. BRE note, 117.
5. Kucera V., Fitz S. (1995). Direct and indirect air pollution effects on materials including cultural monuments. Water Air Soil Poll, 85, 153-165.
6. Kucera V., Tidblad J., Kreislova K., Knotkova D, Faller M., Reiss R., Snethlage R., Yates T., Henriksen J., Schreiner M., Melcher M., Ferm M., Lefèvre R.-A., Kobus J. UN/ECE ICP Materials Dose-response functions for the multi pollutant situation, Acid Rain – Deposition to Recovery (2007) 249-258.
7. Lipfert F.W., Atmospheric damage to calcareous stones: comparison and reconciliation of recent experimental findings, Atmospheric Environment 23 (1989) 415-429.

8. Livingston R.A., Baer N.S., Use of tombstones in investigation of deterioration of stone monument. Environmental Geology and Water Sciences, 16-1 (1990) 83-90.
9. Martínez-Martínez J., Benavente D., Jiménez Gutiérrez S., García-del-Cura M.A., Ordóñez S., Stone weathering under Mediterranean semiarid climate in the fortress of Nueva Tabarca island (Spain) Building Environment 121 (2017) 262-276. https://doi.org/10.1016/j.buildenv.2017.05.034.
10. Reddy M.M., Sherwood S., Doe B., Limestone and marble dissolution by acid rain. In Material and Degradation Caused by Acid Rain ed. R. Baboian, American Chemical Society, Washintgton DC (1986) 226-238.
11. Salvini S. PhD Thesis. Deterioration of carbonate rocks and vulnerability of cultural heritage in a changing climate, Università degli Studi di Padova, 2017.
12. Weber J. (1985). Natural and artificial weathering of Austrian building stones due to air pollution. In: Ve congres international sur l'alteration et la conservation de la pierre. Actes. Vth international congress on deterioration and conservation of stone. Proceedings, Lausanne, 25-27September 1985. Ed. Presses polytechniques romandes, Lausanne, pp. 527-535.
13. Webb A.H., Bawden R.J., Busby A.K., Hopkins J.N., Studies on the effects of air pollution on limestone degradation in Great Britain, Atmospheric Environment, Part B Urban Atmosphere 26 (1992) 165-181. https://doi.org/10.1016/0957-1272(92)90020-S.
14. Yerrapragada S.S., Chirra S.R., Jaynes J.H., Li S., Bandyopadhyay J.K., Gauri K.L., Srinivas B., Surendra S.Y., Weathering rates of marble in laboratory and outdoor conditions, Journal of Environmental Engeneering 122 (1996) 856-863. https://doi.org/10.1061/(ASCE)0733-9372(1996)122:(856).